CRYSTAL GROWTH & DESIGN

ARTICLE

pubs.acs.org/crystal

Syntheses, Crystal Structures, and Luminescence Properties of Three Novel Lead Carboxyphosphonates with 3D Framework Structures Using Rigid Aromatic Carboxylic Acids as Second Organic Ligands

Kai Chen,[†] Zhen-Gang Sun,*[,†] Yan-Yu Zhu,[†] Zhong-Min Liu,[‡] Fei Tong,[†] Da-Peng Dong,[†] Jing Li,[†] Cheng-Qi Jiao,[†] Chao Li,[†] and Cheng-Lin Wang[†]

[†]Institute of Chemistry for Functionalized Material, School of Chemistry and Chemical Engineering, Liaoning Normal University, Dalian 116029, People's Republic of China

[‡]Dalian Institute of Chemical Physics, Chinese Academy of Sciences, Dalian 116023, People's Republic of China

Supporting Information

ABSTRACT: By introduction of three differently structured rigid aromatic carboxylic acids as second organic ligands, three novel lead(II) carboxyphosphonates with 3D framework structures, namely, $[Pb_4(HL)(bts)_2(H_2O)]\cdot 2H_2O$ (**1**), $[Pb_4(HL)(L)(bdc)_{1.5}]\cdot 2H_2O$ (**2**), and $[Pb_3(HL)_2(Hssc)]\cdot 2H_2O$ (**3**) ($H_3L = H_2O_3PCH_2-NC_5H_9-COOH$, $NaH_2bts = NaO_3SC_6H_3(COOH)_2$, $H_2bdc = HOOCC_6H_4COOH$, $H_3ssc = HOOCC_6H_3(SO_3H)(OH)$), have been synthesized under hydrothermal conditions and structurally characterized. The structure of compound **1** features a 3D network built by the cross-linking of 1D double chains of lead(II) phosphonates and 2D layers of lead(II) carboxylate-sulfonate. Compound **2** exhibits a 3D structure built up from Pb^{II} polyhedra, carboxyphosphonates, and bdc^{2-} ions. The structure of compound **3** can be described as a 3D framework type. The $Pb(1)O_6$, $Pb(2)O_4$, $Pb(3)O_5$, and CPO_3 polyhedra are interconnected to form infinite double chain and the second linkers are hung in this chain, which is further connected to adjacent chains through carboxyphosphonate ligands to form a 3D framework structure. The luminescence properties of compounds **1**−**3** have also been studied.

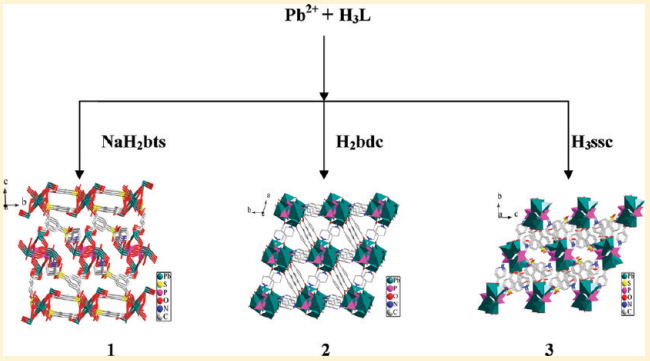

INTRODUCTION

Metal phosphonate compounds with unusual structures and properties are attracting increasing attention not only for their interesting molecular topologies but also for their potential applications as functional materials in the areas of catalysis, ion exchange, proton conductivity, intercalation chemistry, photochemistry, and materials chemistry.[1]

Therefore, the rational design and assembly of novel metal phosphonates with the intriguing diversity of the architectures and properties has become a particularly important subject.[2] The key factor is the selection of multifunctional phosphonic acid ligands for assembling metal ions to fabricate a desired framework. Much work of metal phosphonates has shown that the use of bi- and multifunctional phosphonic acids containing $-NH_2$, $-OH$, and $-COOH$ subfunctional groups may not only result in new structural types of metal phosphonates but also bring interesting properties. In recent years, a number of metal phosphonate frameworks with additional functionality have been reported.[3] By attaching functional groups such as amine, hydroxyl, and carboxylate groups to the phosphonic acid, a series of metal phosphonates with a framework structure have also been isolated in our laboratory.[4] Recently, many research activities have concerned with the synthesis of hybrid frameworks by incorporating a second organic ligands such as oxalate, carboxylic acid, sulfonic acids, 2, 2′-bipyridine, 4, 4′-bipyridine, or 1, 10-phenanthroline into the structures of metal phosphonates.[5] Results from ours and other groups indicate that the introduction of a second ligand has been found to be an effective synthetic method in the synthesis of metal phosphonates, since these molecules can act as pillars between neighboring layers or be grafted into the inorganic layer to form new hybrid architectures.[6] Although great efforts have been made in the construction of hybrid frameworks by introducing an acidic metal linker into the structures of metal phosphonates, very few compounds are concerned with the use of rigid aromatic carboxylic acids forming part of the structure with phosphonate groups.[7] More recently, two new Zn(II) and Cd(II) phosphonates with a 3D framework structure have been obtained by our group by using the 1,4-benzenedicarboxylic acid (H_2bdc) as the second organic ligand.[8] The chelating effect of aromatic carboxylic acids usually leads to metal phosphonates

Received: July 11, 2011
Revised: August 30, 2011
Published: September 01, 2011

dx.doi.org/10.1021/cg200876t | *Cryst. Growth Des.* 2011, 11, 4623–4631

with higher dimensionalities. Their relatively rigid structures and the π-conjugated character are more useful to produce coordination polymers with active photoluminescent properties. In the present paper, by employing carboxyphosphonic acid, $H_2O_3PCH_2-NC_5H_9-COOH$ (H_3L) as the phosphonate ligands and three differently structured rigid aromatic carboxylic acids such as 5-sulfoisophthalic acid monosodium salt (NaH_2bts), 1,4-benzenedicarboxylic acid (H_2bdc), and 5-sulfosalicylic acid (H_3ssc) as the second metal linkers, we have successfully prepared three novel lead carboxyphosphonate hybrids with a 3D framework structures, namely, $[Pb_4(HL)(bts)_2(H_2O)]\cdot 2H_2O$ (**1**), $[Pb_4(HL)(L)(bdc)_{1.5}]\cdot 2H_2O$ (**2**), and $[Pb_3(HL)_2(Hssc)]\cdot 2H_2O$ (**3**) The luminescence properties of compounds **1**−**3** have also been studied.

EXPERIMENTAL SECTION

Materials and Methods. The carboxyphosphonic acid, $H_2O_3PCH_2-NC_5H_9-COOH$ (H_3L) was prepared by a Mannich-type reaction according to procedures described previously.[9] All other chemicals were used as obtained without further purification. C, H, and N were determined by using a PE-2400 elemental analyzer. P and Pb were determined by using an inductively coupled plasma (ICP) atomic absorption spectrometer. IR spectra were recorded on a Bruker AXS TENSOR-27 FT-IR spectrometer with KBr pellets in the range of 4000−400 cm^{-1}. The X-ray powder diffraction data was collected on a Bruker AXS D8 Advance diffractometer using Cu Kα radiation (λ = 1.5418 Å) in the 2θ range of 5−60° with a step size of 0.02° and a scanning rate of 3°/min. Thermogravimetric (TG) analyses were performed on a Perkin−Elmer Pyris Diamond TG-DTA thermal analyses system in static air with a heating rate of 10 K min^{-1} from 50 to 900 °C. The luminescence spectra were reported on a HITACHI F-4600 spectrofluorimeter (solid).

*Synthesis of $[Pb_4(HL)(bts)_2(H_2O)]\cdot 2H_2O$ (**1**).* A mixture of $Pb(Ac)_2\cdot 3H_2O$ (0.29 g, 0.75 mmol), H_3L (0.07 g, 0.25 mmol), and NaH_2bts (0.14 g, 0.5 mmol) was dissolved in 10 mL of distilled water. The resulting solution was stirred for about 1 h at room temperature, sealed in a 20-mL Teflon-lined stainless steel autoclave, and heated at 140 °C for 3 days under autogenous pressure. After the mixture was cooled slowly to room temperature, the colorless block crystals were obtained in ca. 33.6% yield based on Pb. Initial pH 3.5. Final pH 4.0. Anal. Calcd for $C_{23}H_{24}NO_{22}PPb_4S_2$: C, 17.37; H, 1.52; N, 0.88; P, 1.95; Pb, 52.11. Found: C, 17.32; H, 1.58; N, 0.83; P, 1.91; Pb, 52.18%. IR (KBr, cm^{-1}): 3371 m, 3070 m, 2930 w, 2844 w, 1605 s, 1540 s, 1443 s, 1357 s, 1206 s, 1153 s, 1031 s, 965 s, 725 s, 626 s, 551 m, 435 m.

*Synthesis of $[Pb_4(HL)(L)(bdc)_{1.5}]\cdot 2H_2O$ (**2**).* A mixture of $Pb(NO_3)_2$ (0.17 g, 0.5 mmol), H_3L (0.39 g, 1.5 mmol), and H_2bdc (0.32 g, 2 mmol) was dissolved in 8.0 mL of deionized water. The pH value was adjusted to 4.0 by adding 2 M aqueous NaOH dropwise. The resulting solution was stirred for about 1 h at room temperature, sealed in a 20-mL Teflon-lined stainless steel autoclave, and heated at 180 °C for 3 days under autogenous pressure. After the mixture was cooled slowly to room temperature, the colorless block crystals were obtained in ca. 52.6% yield based on Pb. Initial pH 4.0. Final pH 4.5. Anal. Calcd for $C_{26}H_{33}N_2O_{18}P_2Pb_4$: C, 20.12; H, 2.14; N, 1.80; P, 3.99; Pb, 53.39. Found: C, 20.18; H, 2.08; N, 1.75; P, 3.92; Pb, 53.48%. IR (KBr, cm^{-1}): 3423 m, 3040 w, 2940 w, 1543 s, 1380 s, 1104 s, 1056 s, 965 s, 824 m, 750 m, 621 w, 543 s, 450 w.

*Synthesis of $[Pb_3(HL)_2(Hssc)]\cdot 2H_2O$ (**3**).* A mixture of $Pb(Ac)_2\cdot 3H_2O$ (0.30 g, 0.75 mmol), H_3L (0.14 g, 0.5 mmol), and H_3ssc (0.13 g, 0.5 mmol) was dissolved in 10.0 mL of deionized water. The pH value was adjusted to 4.0 by adding 2 M aqueous NaOH dropwise. The resulting solution was stirred for about 1 h at room temperature, sealed in a 20-mL Teflon-lined stainless steel autoclave, and heated at 180 °C for 3 days under autogenous pressure. After the mixture was cooled slowly to room temperature, the colorless block crystals were obtained in ca. 45.5% yield based on Pb. Initial pH 4.0. Final pH 4.5. Anal. Calcd for $C_{21}H_{32}N_2O_{18}P_2Pb_3S$: C, 19.16; H, 2.45; N, 2.13; P, 4.71; Pb, 47.23. Found: C, 19.11; H, 2.40; N, 2.18; P, 4.65; Pb, 47.28%. IR (KBr, cm^{-1}): 3459 s, 3133 w, 3003 w, 2947 w, 2733 w,1568 s, 1434 s, 1328 m, 1263 m, 1217 w, 1179 w, 1086 s, 966 s, 742 m, 671 m, 598 s, 550 s, 477 w .

Table 1. Crystal Data and Structure Refinement for 1−3

compounds	1	2	3
Fw	1590.28	1552.24	1316.06
color and habit	colorless, block	colorless, block	colorless, block
space group	$P-1$	$P-1$	$P2(1)/c$
a (Å)	10.2666(13)	11.727(3)	10.8620(11)
b (Å)	10.3149(13)	12.652(3)	21.225(2)
c (Å)	17.344(2)	13.879(3)	13.8575(14)
α (deg)	90.127(2)	95.064(3)	90
β (deg)	94.382(2)	105.759(3)	96.1050(10)
γ (deg)	117.484(2)	104.946(3)	90
V (Å^3)	1623.2(4)	1886.9(7)	3176.7(6)
Z	2	2	4
T (K)	293	293	293
λ (Å)	0.71073	0.71073	0.71073
D_c (g cm^{-3})	3.254	2.732	2.752
μ (mm^{-1})	20.957	17.952	16.110
R_1, wR_2 (for $I > 2\sigma(I)$)[a]	0.0438, 0.0940	0.0558, 0.1358	0.0480, 0.0936
R_1, wR_2 (for all data)	0.0636, 0.1027	0.0883, 0.1551	0.0867, 0.1099

[a] $R_1 = \Sigma(|F_0|-|F_C|)/\Sigma|F_0|$, $wR_2 = [\Sigma w(|F_0|-|F_C|)^2/\Sigma wF_0^2]^{1/2}$.

X-ray Crystallography. Data collections for compounds **1**−**3** were performed on the Bruker AXS Smart APEX II CCD X diffractometer equipped with graphite monochromated Mo Kα radiation (λ = 0.71073 Å) at 293 ± 2 K. An empirical absorption correction was applied using the SADABS program. The structures were solved by direct methods and refined by full matrix least-squares on F^2 by using the programs SHELXS-97.[10] All non-hydrogen atoms were refined anisotropically. Hydrogen atoms except those for water molecules were generated geometrically with fixed isotropic thermal parameters, and included in the structure factor calculations. Hydrogen atoms for water molecules were not included in the refinement. Details of crystallographic data of compounds **1**−**3** are summarized in Table 1. Selected bond distances and angles of compounds **1**−**3** are listed in Tables 2′−4. Hydrogen bonds for compounds **1** and **3** are listed in Table 5.

RESULTS AND DISCUSSION

Syntheses. Three novel lead(II) carboxyphosphonates with different types of 3D framework structures have been synthesized under hydrothermal conditions, using $H_2O_3PCH_2-NC_5H_9-COOH$ (H_3L) as the phosphonate ligand and three differently structured rigid aromatic carboxylic acids such as 5-sulfoisophthalic acid monosodium salt (NaH_2bts), 1,4-benzenedicarboxylic acid (H_2bdc), and 5-sulfosalicylic acid (H_3ssc) as the second ligands. With the aim to obtain pure phase materials we try to adjust the synthetic conditions of compounds **1**−**3**. It is found that the molar ratio of starting materials plays a key role in the formation of three compounds. Larger crystals of compound **1** were obtained in regions with the molar ratio $Pb^{2+}/H_3L/NaH_2bts$ = 3:1:2. Compound **2** was obtained as larger crystals with the molar ratio $Pb^{2+}/H_3L/H_2bdc$ = 1:3:4, whereas microcrystalline powder was mainly obtained with the molar ratio $Pb^{2+}/H_3L/H_2bdc$ = 4:1:1.5. The best crystallinity of compound **3** was isolated with the molar ratio $Pb^{2+}/H_3L/H_3ssc$ = 3:2:2. In addition, the pH value was very

dx.doi.org/10.1021/cg200876t |Cryst. Growth Des. 2011, 11, 4623–4631

Table 2. Selected Bond Distances (Å) and Angles (deg) for 1[a]

distances (Å)			
Pb(1)−O(12)#1	2.541(8)	Pb(3)−O(2)	2.364(8)
Pb(1)−O(9)#2	2.552(8)	Pb(3)−O(19)	2.417(7)
Pb(1)−O(16)	2.567(8)	Pb(3)−O(18)	2.677(8)
Pb(1)−O(17)#3	2.570(8)	Pb(4)−O(1)	2.364(8)
Pb(1)−O(17)	2.606(9)	Pb(4)−O(4)#7	2.378(8)
Pb(1)−O(6)#4	2.609(8)	Pb(4)−O(3)#6	2.597(7)
Pb(1)−O(7)	2.695(7)	Pb(4)−O(20)	2.616(9)
Pb(2)−O(10)#5	2.394(7)	Pb(4)−O(5)#7	2.706(8)
Pb(2)−O(11)	2.458(8)	P(1)−O(1)	1.506(8)
Pb(2)−O(7)#1	2.533(8)	P(1)−O(2)	1.520(8)
Pb(2)−O(12)	2.743(8)	P(1)−O(3)	1.520(7)
Pb(3)−O(3)#6	2.360(8)	P(1)−C(1)	1.836(13)
angles (deg)			
O(12)#1−Pb(1)−O(9)#2	161.6(3)	O(10)#5−Pb(2)−O(12)	125.3(3)
O(2)−Pb(3)−O(18)	121.5(3)	O(1)−Pb(4)−O(5)#7	119.9(3)

[a] Symmetry transformations used to generate equivalent atoms. For **1**: #1, $-x+1, -y+1, -z+1$; #2, $x, y-1, z$; #3, $-x+1, -y, -z+1$; #4, $-x, -y, -z+1$; #5, $x+1, y, z$; #6, $-x+2, -y, -z$; #7, $-x+3, -y, -z$.

Table 3. Selected Bond Distances (Å) and Angles (deg) for 2[a]

distances (Å)			
Pb(1)−O(2)#1	2.278(12)	Pb(3)−O(10)#6	2.755(12)
Pb(1)−O(9)#2	2.334(13)	Pb(4)−O(15)	2.351(14)
Pb(1)−O(13)#3	2.479(13)	Pb(4)−O(12)#6	2.375(12)
Pb(1)−O(1)	2.529(11)	Pb(4)−O(10)	2.391(10)
Pb(2)−O(3)#4	2.277(11)	P(1)−O(3)	1.508(11)
Pb(2)−O(6)	2.412(12)	P(1)−O(1)	1.517(11)
Pb(2)−O(5)	2.577(15)	P(1)−O(2)	1.534(12)
Pb(2)−O(8)#5	2.746(15)	P(1)−C(1)	1.828(17)
Pb(3)−O(11)	2.315(11)	P(2)−O(11)	1.515(12)
Pb(3)−O(16)#6	2.476(12)	P(2)−O(12)	1.516(12)
Pb(3)−O(14)#7	2.479(14)	P(2)−O(10)	1.536(10)
Pb(3)−O(4)	2.620(12)	P(2)−C(16)	1.815(17)
angles (deg)			
O(9)#2−Pb(1)−O(1)	110.6(5)	O(11)−Pb(3)−O(16)#6	107.0(5)
O(4)−Pb(3)−O(10)#6	116.2(4)	O(15)−Pb(4)−O(12)#6	87.7(4)

[a] Symmetry transformations used to generate equivalent atoms. For **2**: #1, $-x+3, -y+1, -z+1$; #2, $-x+3, -y+2, -z+1$; #3, $x+1, y+1, z+1$; #4, $-x+2, -y+1, -z+1$; #5, $-x+2, -y+2, -z+1$; #6, $-x+1, -y+1, -z$; #7, $-x+1, -y, -z$.

important for the formation of suitable single crystals for X-ray diffraction. NaOH was added into the reaction system in the form of solution, which was employed as the inorganic base to adjust the pH of the reaction mixture. The initial and final pH values of the resultant solution are about 3.5 and 4.0 for compound **1** and 4.0 and 4.5 for compounds **2** and **3**, respectively. The powder X-ray diffraction patterns (PXRD) of compounds **1**−**3** all match those simulated from single-crystal X-ray data (Figures S7−S9 of Supporting Information).

Crystal Structures of $[Pb_4(HL)(bts)_2(H_2O)]\cdot 2H_2O$ (1). Compound **1** crystallizes in the triclinic space group $P\bar{1}$. The

Table 4. Selected Bond Distances (Å) and Angles (deg) for 3[a]

distances (Å)			
Pb(1)−O(5)#1	2.546(9)	Pb(3)−O(10)#5	2.427(9)
Pb(1)−O(2)	2.574(8)	Pb(3)−O(15)	2.630(11)
Pb(1)−O(9)#2	2.601(9)	Pb(3)−O(6)#6	2.631(8)
Pb(1)−O(1)#3	2.612(8)	Pb(3)−O(3)	2.730(8)
Pb(1)−O(8)#4	2.624(8)	P(1)−O(1)	1.518(8)
Pb(1)−O(4)#1	2.637(9)	P(1)−O(3)	1.514(9)
Pb(2)−O(3)	2.400(9)	P(1)−O(2)	1.518(8)
Pb(2)−O(4)#1	2.456(10)	P(1)−C(1)	1.821(11)
Pb(2)−O(1)#3	2.652(8)	P(2)−O(8)	1.493(9)
Pb(2)−O(13)#1	2.787(14)	P(2)−O(6)	1.521(9)
Pb(2)−O(2)#3	2.746(8)	P(2)−O(7)	1.537(9)
Pb(3)−O(7)	2.298(9)	P(2)−C(8)	1.852(12)
angles (deg)			
O(2)−Pb(1)−O(8)#4	124.7(3)	O(4)#1−Pb(2)−O(2)#3	115.7(3)
O(7)−Pb(3)−O(6)#6	100.4(3)		

[a] Symmetry transformations used to generate equivalent atoms. For **3**: #1, $x, -y+{}^1/_2, z-{}^1/_2$; #2, $x+1, -y+{}^1/_2, z+{}^1/_2$; #3, $-x+2, -y, -z+1$; #4, $x+1, y, z$; #5, $x, -y+{}^1/_2, z+{}^1/_2$; #6, $-x+1, -y, -z+1$.

Table 5. Hydrogen Bonds for Compounds 1 and 3

D−H···A	D(D−H)/ Å	d(H···A)/ Å	D−H−A/ deg	d(D···A)/ Å
compound **1**				
O20−H20B···O1W	0.85	2.23	122.9	2.788(18)
O20−H20A···O15	0.85	2.04	144.0	2.777(12)
O1W−H1WA···O2	0.85	2.32	149.8	3.080(16)
O2W−H2WB···O16	0.85	2.07	144.6	2.804(13)
compound **3**				
O1W−H1WB···O14	0.85	2.10	134.0	2.761(18)
O2W−H2WB···O12	0.85	2.34	136.4	3.012(19)

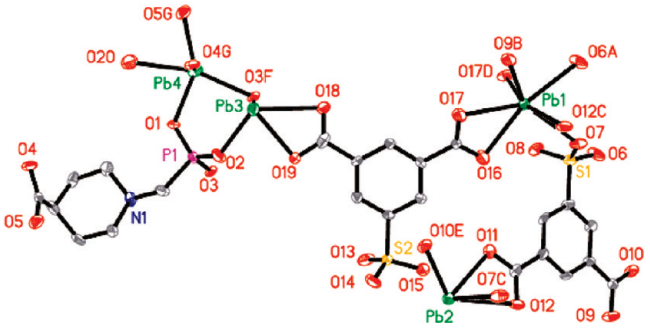

Figure 1. ORTEP representation of a selected unit of compound **1**. The thermal ellipsoids are drawn at the 50% probability level. All H atoms and lattice water molecules are omitted for clarity. Symmetry codes: A: $-x, -y, -z+1$; B: $x, y-1, z$; C: $-x+1, -y+1, -z+1$; D: $-x+1, -y, -z+1$; E: $x+1, y, z$; F: $-x+2, -y, -z$; G: $-x+3, -y, -z$.

structure of compound **1** features a complicated 3D network. The asymmetric unit of compound **1** contains four crystallographically unique Pb(II) ions, one HL^{2-} anion, two bts^{3-} anions, one coordinated water molecule, and two lattice water molecules.

dx.doi.org/10.1021/cg200876t |*Cryst. Growth Des.* 2011, 11, 4623–4631

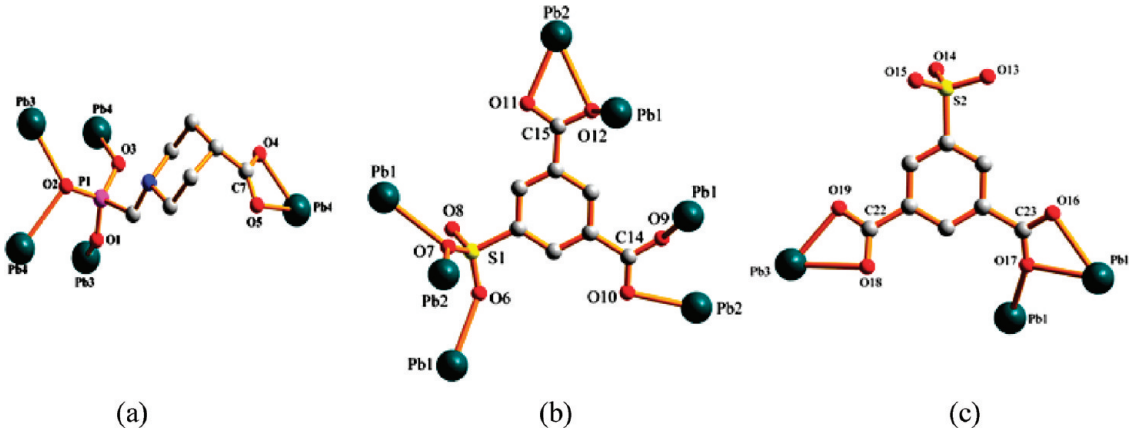

Figure 2. The coordination fashions of H_3L in compound **1** (a). Coordination modes of the 5-sulfoisophthalic acid monosodium salt ligands in compound **1** (b, c).

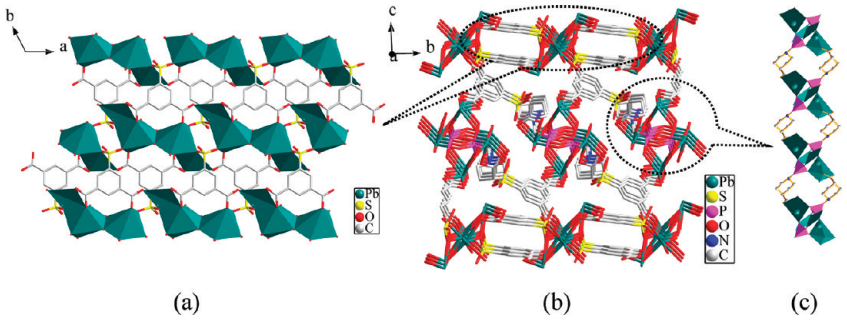

Figure 3. (a) A 2D layer of lead(II) carboxylate−sulfonate of compound **1** viewed in the *ab* plane. (b) View of the framework for compound **1** along the *a* axis. All H atoms are omitted for clarity. (c) A 1D double chain of lead(II) phosphonate along the *a* axis.

As shown in Figure 1, Pb1 ion is seven-coordinated by five carboxylate oxygen atoms (O9B, O12C, O16, O17, and O17D) from four bts^{3-} anions and two sulfonate oxygen atoms (O6 and O7) from two bts^{3-} anions. Pb2 ion is four-coordinated by three carboxylate oxygen atoms (O10E, O11, and O12) from two bts^{3-} anions and one sulfonate oxygen atom (O7C) from one bts^{3-} anion. Pb3 ion is also four-coordinated by two carboxylate oxygen atoms (O18 and O19) from one bts^{3-} anion and two phosphonate oxygen atoms (O2 and O3F) from two HL^{2-} anions. Pb4 ion is five-coordinated by two carboxylate oxygen atoms (O4G and O5G) from one HL^{2-} anion, two phosphonate oxygen atoms (O1 and O3F) from two HL^{2-} anions, and one oxygen atom (O20) from a water molecule. The Pb−O bond lengths are in the range of 2.359(8)−2.742(8) Å, which are comparable to those reported for other lead(II) phosphonates.[11] On the basis of the requirement of charge balance as well as P−O, C−O, and S−O distances, the amino group of the phosphonate ligand is protonated. As shown in Figure 2a, the coordination mode of the HL^{2-} anion can be described as a hexadentate bridging mode. It chelates one Pb(4) ion through two carboxylate oxygen atoms (O4 and O5). The phosphonate oxygen atom (O2) is bidentately bridging, whereas the remaining phosphonate oxygen atoms (O1 and O3) are unidentate. The bts^{3-} anion containing O6 to O12 is octadentate and bridges seven Pb(II) ions (Figure 2b). The sulfonate group of S1O6O7O8 bridges three Pb(II) ions (three bonds to two Pb1 atoms and one Pb2 atom), and O8 is noncoordinated. The carboxylate group C14O9O10 bridges Pb1 and Pb2. The one composed of C15O11O12 forms three bonds, a chelate to one Pb2 atom and a bridge between the Pb1 and Pb2 atom. The second bts^{3-} anion containing O13 to O19 is pentadentate and bridges three Pb(II) ions (Figure 2c). The sulfonate group S2O13O14O15 is noncoordinated. One carboxylate group C22O18O19 is bidentate chelating, whereas the other one composed of C23O16O17 is μ_3 chelating and bridging.

As shown in Figure 3a, $Pb(1)O_7$ and $Pb(2)O_4$ polyhedra are interconnected into a dimer via edge sharing. Two so-built dimers are interconnected into a tetramer via edge sharing. The interconnection of such tetramers by bridging and chelating bts^{3-} anions leads to a 2D layer in *ab* plane. The interconnection of $Pb(3)O_4$, $Pb(4)O_5$, and CPO_3 polyhedra via corner sharing forms a tetranuclear cluster, and such neighboring tetranuclear clusters are further connected through carboxyphosphonate ligands to form a 1D double chain along the *a* axis (Figure 3c). The cross−linking of the above two building units resulted in a 3D network (Figure 3b). Compound **1** has intermolecular hydrogen bonds, such as O20−H20B···O1W, O20−H20A···O15, O1W−H1WA···O2, O2W−H2WB···O16. The corresponding distances are 2.788(18) Å, 2.777(12), 3.080(16) Å, 2.804(13) Å, and the angles are 122.9, 144.0, 149.8,144.6°. These hydrogen bonds can enhance the stability of this network. Although the phenyl rings between the neighboring layers are almost parallel to each other, the close contact distance between adjacent phenyl rings is not in the normal range (3.3−3.8 Å) for such interactions. There are no $\pi-\pi$ stacking interactions in the network of compound **1**.

Crystal Structures of $[Pb_4(HL)(L)(bdc)_{1.5}]\cdot 2H_2O$ (2). The structure of compound **2** also features a complicated 3D network.

dx.doi.org/10.1021/cg200876t |*Cryst. Growth Des.* 2011, 11, 4623–4631

Each asymmetric unit contains four crystallographically independent Pb(II) ions, one HL^{2-} anion, one L^{3-} anion, one bdc^{2-} anion, one half-occupied bdc^{2-} moiety, and two lattice water molecules. As shown in Figure 4, Pb1 ion is four-coordinated by one carboxylate oxygen atom (O9B) from one bdc^{2-} anion and one carboxylate oxygen atom (O13C) from one L^{3-} anion and two phosphonate oxygen atoms (O1 and O2A) from two HL^{2-} anions. Pb2 ion is also four-coordinated by two carboxylate oxygen atoms (O6 and O8E) from two bdc^{2-} anions and one carboxylate oxygen atom (O5) from one HL^{2-} anion and one phosphonate oxygen atom (O3D) from one HL^{2-} anion. Pb3 ion is five-coordinated by one carboxylate oxygen atom (O16F) from one bdc^{2-} anion and one carboxylate oxygen atom (O4) from one HL^{2-} anion and one carboxylate oxygen atom (O14G) from one L^{3-} anion and two phosphonate oxygen atoms (O10F and O11) from two L^{3-} anions. Pb4 ion is three-coordinated by one carboxylate oxygen atom (O15) from one bdc^{2-} anion and two phosphonate oxygen atoms (O10 and O12F) from two L^{3-} anions. The Pb−O bond lengths are in the range of 2.277-(11)−2.755(12) Å, which are comparable to those reported for other lead(II) phosphonates.[12] The coordination modes of the two H_3L ligands can be described as pentadentate and hexadentate

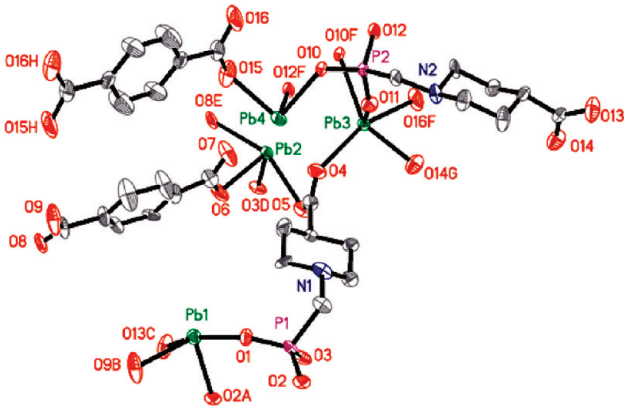

Figure 4. ORTEP representation of a selected unit of compound **2**. The thermal ellipsoids are drawn at the 50% probability level. All H atoms and lattice water molecules are omitted for clarity. Symmetry codes: A: $-x+3, -y+1, -z+1$; B: $-x+3, -y+2, -z+1$; C: $x+1, y+1, z+1$; D: $-x+2, -y+1, -z+1$; E: $-x+2, -y+2, -z+1$; F: $-x+1, -y+1, -z$; G: $-x+1, -y, -z$.

bridging modes. As shown in Figure 5a, the HL^{2-} anion which contains P1 atom bridges five Pb(II) ions (two Pb(1), two Pb(2), and one Pb(3)) through two carboxylate oxygen atoms (O4 and O5) and three phosphonate oxygen atoms (O1, O2, and O3). The L^{3-} anion containing P2 serves as a hexadentate ligand, binding six Pb atoms through three phosphonate oxygens (O10, O11, and O12) and two carboxylate oxygens (O13 and O14) (Figure 5b). The two phosphonate oxygen atoms (O11 and O12) of the phosphonate group are monodentate and the third phosphonate oxygen atom (O10) behaves as μ_2 metal linker. The bdc^{2-} anion displays two coordination modes in compound **2**. The first bdc^{2-} anion is a tridentate ligand to one Pb(1) ion and two Pb(2) ions through three carboxylate oxygen atoms (O6, O8 and O9), and O7 is noncoordinated (Figure 5c). The second bdc^{2-} anion is a tetradentate ligand to two Pb(3) and two Pb(4) ions through four carboxylate oxygen atoms (O15, O16, O15H, and O16H) (Figure 5d).

Compound **2** exhibits a 3D structure built up from Pb^{II} polyhedra, carboxyphosphonates, and bdc^{2-} ions (Figure 6a). The $Pb(1)O_4$, $Pb(2)O_4$, and CPO_3 tetrahedra are linked in a corner-sharing manner to form tetranuclear clusters (A). The interconnection of $Pb(3)O_5$, $Pb(4)O_3$, and CPO_3 polyhedra via corner−sharing also forms tetranuclear clusters (B). The cross−linking of the above two building clusters through two carboxylate oxygens (O4 and O5) from HL^{2-} anion forms an inorganic chain running along the *c* axis. Each chain is linked by the coordination of carboxylate oxygen atoms from μ_4-bdc to two Pb(3) and two Pb(4) ions and μ_3-bdc to one Pb(1) and two Pb(2) ions to form a 2D layer (Figure 6b). On the other hand, the above chains are linked by L^{3-} anions giving structural layer (Figure 7a). Neighboring layers are connected through the HL^{2-} anions, leading to a 3D pillared layered structure with 1D channel system along the *c*-axis (Figure 7b). It is different from compound **1**, the hydrogen−bonding interactions are not observed in the structure of compound **2**. The close contact distance between adjacent phenyl rings, which are almost parallel to each other, is not in the normal range (3.3−3.8 Å) for such interactions. So $\pi-\pi$ stacking interactions are not observed in the framework of compound **2** either.

Crystal Structures of $[Pb_3(HL)_2(Hssc)]\cdot 2H_2O$ (3). The structure of compound **3** also features a complicated 3D network. The asymmetric unit consists of the following structural elements: three crystallographically unique Pb(II) ions, two HL^{2-} anions, one $Hssc^{2-}$ anion, and two lattice water molecules. As shown in

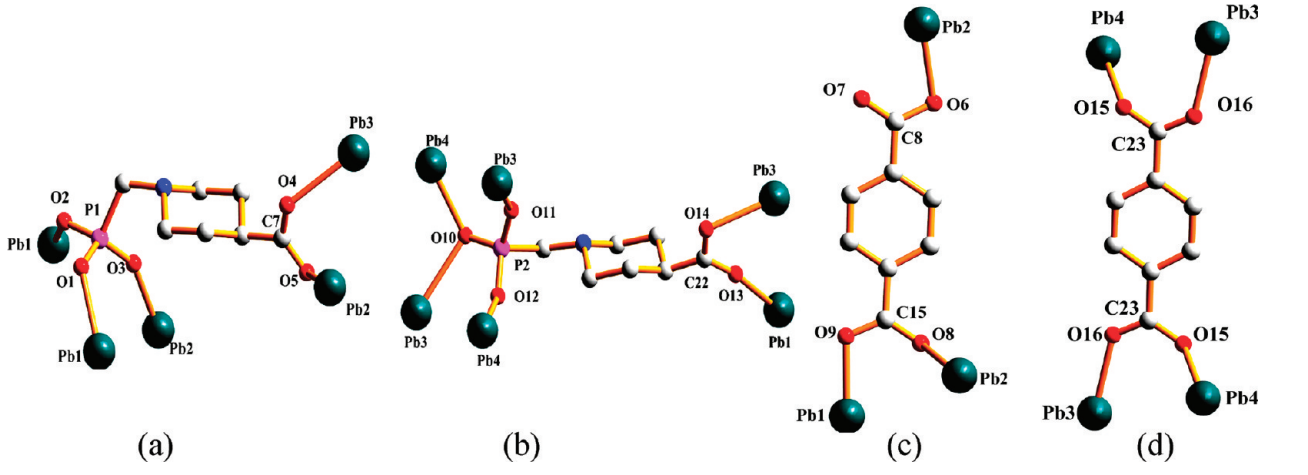

Figure 5. The coordination fashions of H_3L in compound **2** (a, b). Coordination modes of the 1, 4-benzenedicarboxylic acid ligands in compound **2** (c, d).

dx.doi.org/10.1021/cg200876t |*Cryst. Growth Des.* 2011, 11, 4623–4631

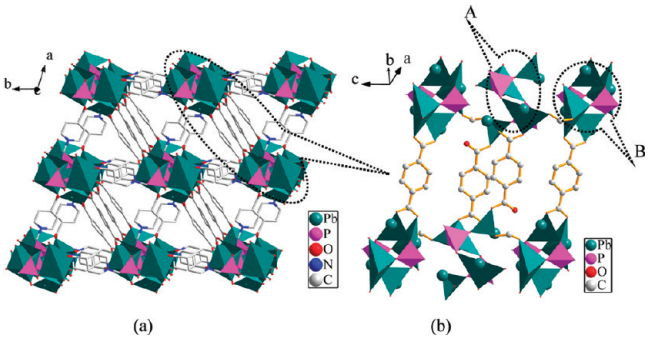

Figure 6. (a) View of the 3D framework for compound **2** along the *c* axis. (b) The inorganic chains linked by bdc^{2-} anions.

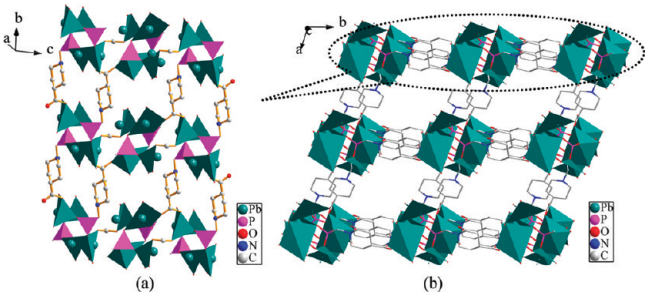

Figure 7. (a) The double layer structure of compound **2**. (b) View of the 3D framework for compound **2** without bdc^{2-} anions.

Figure 8, Pb1 ion is six-coordinated by three carboxylate oxygen atoms (O4B, O5B, and O9D) from two HL^{2-} anions and three phosphonate oxygen atoms (O1A, O2, and O8C) from three different HL^{2-} anions. Pb2 ion is four-coordinated by one carboxylate oxygen atom (O4B) from one HL^{2-} anion and three phosphonate oxygen atoms (O1A, O2A, and O3) from two HL^{2-} anions. Pb3 ion is five-coordinated by one carboxylate oxygen atom (O15) from one $Hssc^{2-}$ anion and one carboxylate oxygen atom (O10F) from one HL^{2-} anion and three phosphonate oxygen atoms (O3, O6E, and O7) from three HL^{2-} anions. The Pb−O bond lengths are in the range of 2.298(9)−2.787(14) Å, which are comparable to those reported for other lead(II) phosphonates.[13] The coordination modes of the two carboxyphosphonate ligands are different. The first ligand, which adopts an interesting coordination mode (Figure 9a), containing P1 atom, bridges seven Pb(II) ions through its three phosphonate oxygen atoms and two carboxyl oxygen atoms. Three phosphonate oxygen atoms (O1, O2, and O3) and carboxylate oxygen atom (O4) act as μ_2 metal linker. The phosphonate group forms a chelate with the Pb2 atom and bridges two Pb1 atoms through two phosphonate oxygen atoms (O1 and O2). The O3 atom of the phosphonate group bridges the Pb2 and the Pb3 atoms. The carboxylate group C7O4O5 forms three bonds, a chelate to one Pb1 atom and a bridge between the Pb1 and the Pb2 atoms. The second ligand, containing P2 atom, serves as a pentadentate ligand, adopting a coordination mode that is the same as L^{3-} anion in compound **2** (Figure 9b). The carboxylate group C15O15O16 of $Hssc^{2-}$ anion is unidentate, and the other groups of $Hssc^{2-}$ anion are noncoordinated (Figure 9c).

The overall structure of compound **3** can be described as a 3D framework type. The $Pb(1)O_6$, $Pb(2)O_4$, and $Pb(3)O_5$ polyhedra are interconnected into a trimer via corner and edge sharing.

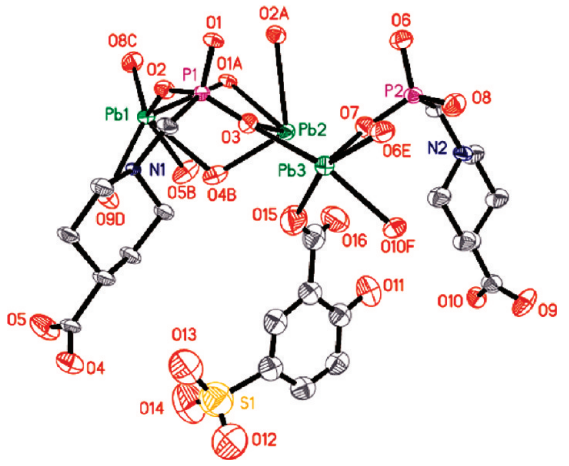

Figure 8. ORTEP representation of a selected unit of compound **3**. The thermal ellipsoids are drawn at the 50% probability level. All H atoms and lattice water molecules are omitted for clarity. Symmetry codes: A: $-x+2, -y, -z+1$; B: $x, -y+{}^1/_2, z-{}^1/_2$; C: $x+1, y, z$; D: $x+1, -y+{}^1/_2, z+{}^1/_2$; E: $-x+1, -y, -z+1$; F: $x, -y+{}^1/_2, z+{}^1/_2$.

Such trimers are linked to each other by CPO_3 tetraheda to form infinite double chains, and the second linkers are hung in this chain (Figure 10a), which is further connected to adjacent chains through carboxyphosphonate ligands to form a 3D open-framework structure (Figure 10b). In other words, the above chains are interconnected by carboxyphosphonate anions to form a 2D inorganic layer (Figure 11a). The adjacent layers are connected through the HL^{2-} anions from one layer to others (Figure 11b). It is interesting to note that the interconnection of Pb1, Pb2, and Pb3 ions by bridging and chelating four carboxyphosphonate anions leads to a 3D network of $\{Pb_3(HL)_4\}^{2-}$ with a 1D channel system along the *a* axis. The channel is formed by 43-membered rings composed of six Pb (II) ions and four carboxyphosphonate anions. There are intermolecular hydrogen bonds among the lattice water molecules and the oxygen atoms from Hssc ligand with the distances of 2.761(18) Å (O1W−H1WB···O14), 3.012(19) Å (O2W−H2WB···O12), and the corresponding angles of 134.0 and 136.4°. These hydrogen bonds enhance the stability of the network. It is similar to compound **1** and **2**, the close contact distance between adjacent phenyl rings is not in the normal range (3.3−3.8 Å) for such interactions, hence there are no $\pi-\pi$ stacking interactions in the network compound **3**.

IR Spectroscopy. The IR spectra for compounds **1**−**3** are recorded in the region 4000−400 cm^{-1}. The absorption band at 3371 cm^{-1} for **1**, 3423 cm^{-1} for **2**, and 3459 cm^{-1} for **3** can be assigned to the O−H stretching vibrations of water molecules. The weak bands at 3070 cm^{-1} for 1, 3040 cm^{-1} for **2**, and 3133 cm^{-1} for **3** are attributed to the N−H stretching vibrations. The C−H stretching vibrations are observed as sharp, weak bands close to 3000 cm^{-1} for compounds **1**−**3**. The bands at 1605, 1540, and 1443 cm^{-1} for **1**, 1543 and 1380 cm^{-1} for **2**, such bands appeared at 1568 and 1434 cm^{-1} for **3** are observed, which are shifted from the excepted value of uncoordinated carboxylic acids [ν(C−O) typically around 1725−1700 cm^{-1}]. These shifts are due to the carboxylate function coordinated to the metal atom, and these bands are assigned to the asymmetric and symmetric stretching vibrations of C−O groups when present as COO^- moieties.[14] The stretching vibration absorption band of the sulfonate group was appeared at 1206 cm^{-1} in

dx.doi.org/10.1021/cg200876t |*Cryst. Growth Des.* 2011, 11, 4623–4631

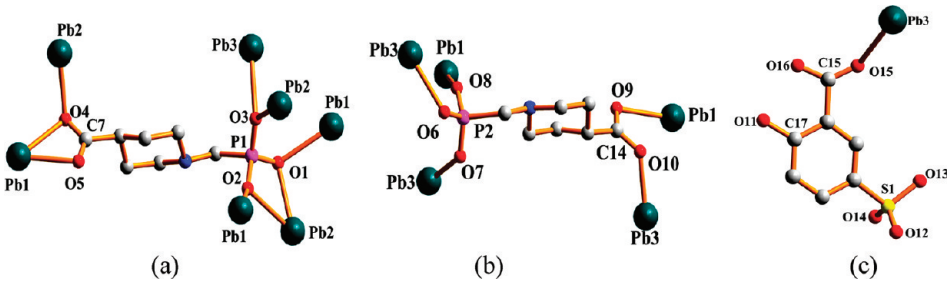

Figure 9. The coordination fashions of H_3L in compound **3** (a, b). Coordination modes of the 5-sulfosalicylic acid ligands in compound **3** (c).

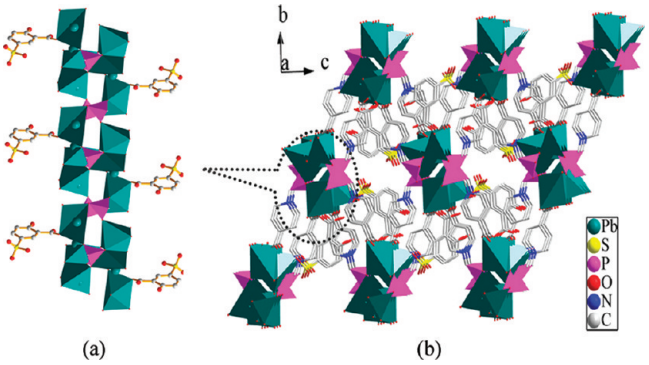

Figure 10. (a) A 1D chain along the *a* axis. (b) View of the 3D framework for compound **3** along the *a* axis.

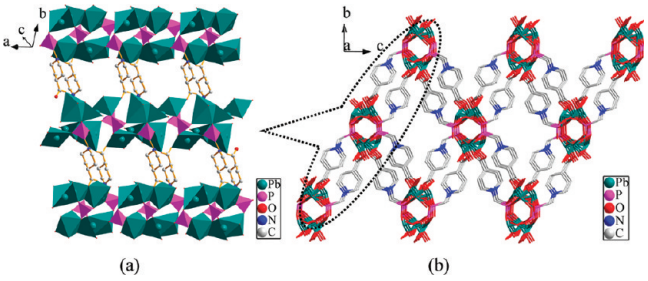

Figure 11. (a) The double-layer structure of compound **3**; (b) 3D network of $\{Pb_3(HL)_4\}^{2-}$ in compound **3**.

compound **1**. The bands at 1263 and 1217 cm^{-1} for compound **3** are attributed to the stretching vibrations of the sulfonate group. Absorption bands around 620 cm^{-1} for **1** and **3** are characteristic bands for ν(S−O) of the sulfonate groups.[15] Strong bands between 1200 and 900 cm^{-1} for three compounds are due to stretching vibrations of the tetrahedral CPO_3 groups,[16] as expected. Additional weak bands at low energy are found. These bands are probably due to bending vibrations of the tetrahedral CPO_3 groups.

Thermal Analysis. To explore the thermal stability of these materials, the TG curves of compounds **1**−**3** were measured. The TG curve of compound **1** shows two main steps of weight losses (Figure S4). The first step started at 50 °C and was completed at 397 °C, which corresponds to the release of two lattice water molecules and one coordinated water molecule. The observed weight loss of 2.8% is close to the calculated value (3.4%). The total weight loss at 900 °C is 32.3%, and the residue was not characterized. The TG curve of compound **2** also exhibits two steps of weight losses (Figure S5). The first step started at 50 °C and was completed at 219 °C, corresponding to the release of two lattice water molecules. The observed weight loss of 2.4% is very close to the calculated value (2.3%). The second step, from 278 to 538 °C, corresponds to decomposition of the organic groups. The observed weight loss of 31.5% is in good agreement with the calculated value (31.1%). The final products are $Pb_2P_2O_7$ and PbO in a 1:2 molar ratio based on XRD powder diffraction (Figure S10). The total weight loss at 800 °C of 33.8% is close to the calculated value (33.4%). The TG curve of compound **3** reveals two steps of weight losses (Figure S6). The first step, in the temperature range 50−161 °C, is due to the removal of two lattice water molecules. The observed weight loss of 3.2% is slightly larger than the theoretical one (2.7%). The second step covers from 284 to 676 °C, corresponding to the decomposition of the organic groups. The observed weight loss of 35.4% is close to the calculated value (35.7%). From powder X−ray diffraction, the final product is identified as $Pb_3(PO_4)_2$ based on XRD powder diffraction (Figure S11). The total weight loss of 38.6% is very close to the calculated value (38.4%). To understand the thermal stability of these compounds, X-ray powder diffraction studies were performed for the as-synthesized compound **1** and the samples heated 180−350 °C, 160−300 °C for compound **2** and 180−250 °C for compound **3** for 2 h under air atmosphere. As shown in Figure S7, the powder XRD patterns demonstrate the retention of framework structure of compound **1** below 300 °C. See Figure S8, at 250 °C, the pattern is similar to that at 25 °C, which indicates that the structure of compound **2** was thermally stable below 250 °C. The powder XRD patterns of compound **3** show as the framework remains stable at 180 °C (Figure S9).

Luminescent Properties. The luminescent behaviors of compounds **1**−**3** were investigated in the solid state at room temperature. The free H_3L ligand shows no emission in the visible region. The free NaH_2bts ligand displays luminescence with an emission maximum at 324 nm (λ_{ex} = 245 nm), while compound **1** exhibits one shoulder weaker emission peak at 462 nm and a broad weaker emission band between 476 and 597 nm with a maximum peak at 504 nm (λ_{ex} = 375 nm) upon complexion of both H_3L and NaH_2bts ligands with the lead(II) ions and the lifetime (λ_{ex} = 375 nm) is 2.3 ms (Figure 12). The free H_2bdc ligand shows a strong fluorescent emission band at 342 nm (λ_{ex} = 307 nm). Upon complexation of both H_3L and H_2bdc ligands with the lead(II) ions, it is intriguing that compound **2** could emit a broad weaker emission band between 447 and 551 nm with the maximum peak at 493 nm (λ_{ex} = 375 nm), and the lifetime (λ_{ex} = 375 nm) is measured to be 4.1 ms (Figure 13). The free H_3ssc ligand exhibits two emission maximum at 369 and 437 nm (λ_{ex} = 274 nm), while compound **3** shows a broad weaker emission

dx.doi.org/10.1021/cg200876t |*Cryst. Growth Des.* 2011, 11, 4623–4631

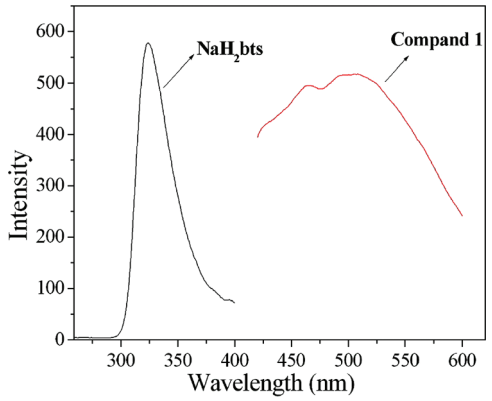

Figure 12. Solid-state emission spectrum of NaH_2bts and compound **1** at room temperature.

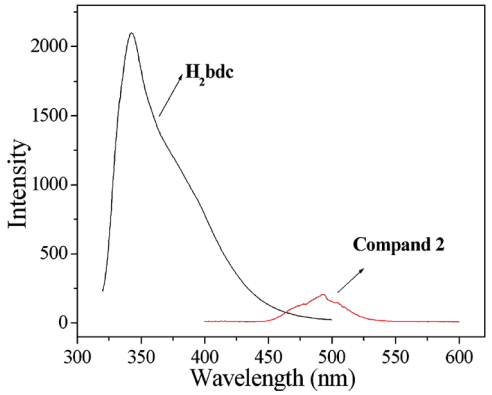

Figure 13. Solid-state emission spectrum of H_2bdc and compound **2** at room temperature.

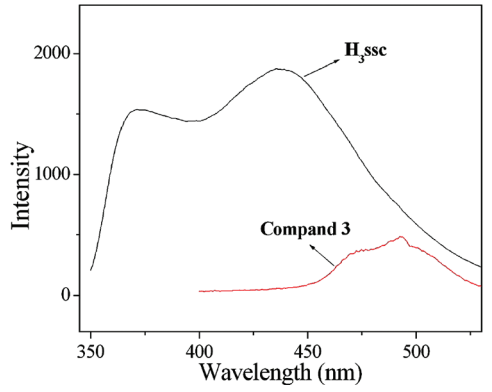

Figure 14. Solid-state emission spectrum of H_3ssc and compound **3** at room temperature.

band between 435 and 529 nm with a maximum peak at 492 nm (λ_{ex} = 375 nm) upon complexion of both H_3L and H_3ssc ligands with the lead(II) ions (Figure 14). Unfortunately, the luminescent lifetime of compound **3** are not observed, since the lifetime of compound **3** is too short to be measured. It is clear that significant red shifts of the emission occur in compounds **1**−**3** compared with the free secondary ligands, which are probably due to the ligand−to−metal charge-transfer (LMCT) transition.[17] These suggests that the emission band of compounds **1**−**3** are mainly attributed to ligand−to−metal charge-transfer emission state as reported for Cd(II) or other d^{10} metal compounds.[18,19] The luminescence spectra of compounds **1**−**3** indicate that the use of the second ligand (NaH_2bts, H_2bdc, and H_3ssc) may be an effective way to prepare luminescent materials.

CONCLUSION

By use of the carboxyphosphonic acid as the phosphonate ligand and three differently structured rigid aromatic carboxylic acids as the second metal linker, three novel lead(II) carboxyphosphonates with different types of 3D framework structures have been successfully synthesized under hydrothermal conditions. Compound **1** features a 3D network built by the cross-linking of 1D double chains of lead(II) phosphonates and 2D layers of lead(II) carboxylate-sulfonate. In compound **2**, the inorganic chains, composed of $Pb(1)O_4$, $Pb(2)O_4$, $Pb(3)O_5$, $Pb(4)O_3$, and CPO_3 polyhedra are interconnected by the carboxyphosphonate and bdc^{2-} acids, thus resulting in a 3D framework structure with 1D channel system along the *c* axis. The structure of compound **3** can be described as a 3D framework type. The $Pb(1)O_6$, $Pb(2)O_4$, $Pb(3)O_5$, and CPO_3 polyhedra are interconnected to form an infinite double chain, and the second linkers are hung in this chain, which is further connected to adjacent chains through carboxyphosphonate ligands to form a 3D framework structure. From the above results, we conclude that introducing aromatic carboxylic acids along with control of reaction conditions is effective in achieving a wide variety of lead(II) carboxyphosphonates structures with higher dimensionalities. In the absence of the second ligands, which usually bind in different bridging modes, three types of 3D framework (compounds **1**−**3**) are obtained. For compound **1**, the dimensionality of the structure is increased when the bts ligand is added as the second metal linker. In compound **2**, the second organic ligands bdc serve as pillars to link the inorganic chains. It is different from compounds **1** and **2**; only the carboxylate group of Hssc ligand is involved in the coordination in compound **3**, and the other organic moieties of Hssc ligand fill in the channel spaces. Thermal stabilities of compounds **1**−**3** have been investigated. Compounds **1**−**3** are stable over a large temperature range up to 300, 250, and 180 °C, respectively. The results of our study indicate that, by introduction of aromatic carboxylic acids as the second ligands, we can obtain lead(II) carboxyphosphonates with good crystals and new structures as well as better luminescence.

ASSOCIATED CONTENT

Supporting Information. X-ray crystallographic files in CIF format for compounds **1**−**3**, IR spectra of compounds **1**−**3**, TG curves of compounds **1**−**3**, XRD patterns of the experiments compared to those simulated from X-ray single-crystal data for compounds **1**−**3** and XRD patterns of the final products in the thermal decomposition for compounds **2** and **3**. CCDC 833187−833189 contain the supplementary crystallographic data for this paper. These data can be obtained free of charge www.ccdc.cam.ac.uk/conts/retrieving.html (or from the Cambridge Crystallographic Data Center, 12 Union Road, Cambridge CB21EZ, United Kindgom. Fax: (+44) 1223−336−033. E-mail: deposit@ccdc.cam.ac.uk). This information is available free of charge via the Internet at http://pubs.acs.org/.

AUTHOR INFORMATION

Corresponding Author
*E-mail: szg188@163.com.

ACKNOWLEDGMENT

This work is supported by the National Natural Science Foundation of China (Grant No. 21071072).

REFERENCES

(1) (a) Clearfield, A. *Chem. Mater.* **1998**, *10*, 2801–2810. (b) Clearfield, A. *Prog. Inorg. Chem.* **1998**, *47*, 371–510. (c) Fanucci, G. E.; Krzystek, J.; Meisel, M. W.; Brunel, L. C.; Talham, D. R. *J. Am. Chem. Soc.* **1998**, *120*, 5469–5479. (d) Kimura, T. *Chem. Mater.* **2003**, *15*, 3742–3744. (e) Maeda, K. *Microporous Mesoporous Mater.* **2004**, *73*, 47–55and references therein..

(2) (a) Groves, J. A.; Miller, S. R.; Warrender, S. J.; Mellot-Draznieks, C.; Lightfoot, P.; Wright, P. A. *Chem. Commun.* **2006**, 3305–3307. (b) Tang, S. F.; Song, J. L.; Li, X. L.; Mao, J. G. *Cryst. Growth Des.* **2007**, *7*, 360–366. (c) Chen, Z. X.; Zhou, Y. M.; Weng, L. H.; Zhao, D. Y. *Cryst. Growth Des.* **2008**, *8*, 4045–4053. (d) Adelani, P. O.; Albrecht-Schmitt, T. E. *Inorg. Chem.* **2009**, *48*, 2732–2734. (e) Taddei, M.; Costantino, F.; Vivani, R. *Inorg. Chem.* **2010**, *49*, 9664–9670.

(3) (a) Habib, H. A.; Gil-Hernández, B.; Abu-Shandi, K.; Sanchiz, J.; Janiak, C. *Polyhedron* **2010**, *29*, 2537–2545. (b) Liu, B.; Li, Y. Z.; Zheng, L. M. *Inorg. Chem.* **2005**, *44*, 6921–6923. (c) Yue, Q.; Yang, J.; Li, G. H.; Li, G. D.; Chen, J. S. *Inorg. Chem.* **2006**, *45*, 4431–4439. (d) Liu, H. Y.; Zhao, B.; Shi, W.; Zhang, Z. J.; Cheng, P.; Liao, D. Z.; Yan, S. P. *Eur. J. Inorg. Chem.* **2009**, 2599–2602. (e) Xu, X. Z.; Wang, P.; Hao, R.; Gan, M.; Sun, F. X.; Zhu, G. S. *Solid State Sci.* **2009**, *6*, 295–300. (f) Pereira, G. A.; Perters, J. A.; Almeida Paz, F. A.; Rocha, J.; Geraldes, C. F. G. C. *Inorg. Chem.* **2010**, *49*, 2969–2974.

(4) (a) Tong, F.; Zhu, Y. Y.; Sun, Z. G.; Wang, W. N.; Zhao, Y.; Lu, X.; Gong, J. *Inorg. Chim. Acta* **2011**, *368*, 200–206. (b) Dong, D. P.; Sun, Z. G.; Tong, F.; Zhu, Y. Y.; Chen, K.; Jiao, C. Q.; Wang, C. L.; Li, C.; Wang, W. N. *CrystEngComm.* **2010**, *13*, 3317–3320. (c) Zhang, N.; Sun, Z. G.; Zhu, Y. Y.; Zhang, J.; Liu, L.; Huang, C. Y.; Lu, X.; Wang, W. N.; Tong, F. *New J. Chem.* **2010**, *34*, 2429–2435. (d) Zhu, Y. Y.; Li, J.; Sun, Z. G.; Zhang, J.; Zhao, Y.; Zhang, N.; Liu, L.; Lu, X. *Inorg. Chem. Commun.* **2009**, *12*, 38–40. (e) Zhang, J.; Li, J.; Sun, Z. G.; Hua, R. N.; Zhu, Y. Y.; Zhao, Y.; Zhang, N.; Liu, L.; Lu, X.; Wang, W. N.; Tong, F. *Inorg. Chem. Commun.* **2009**, *12*, 276–279. (f) Dong, D. P.; Li, J.; Sun, Z. G.; Zheng, X. F.; Chen, H.; Meng, L.; Zhu, Y. Y.; Zhao, Y.; Zhang, J. *Inorg. Chem. Commun.* **2007**, *10*, 1109–1112.

(5) (a) Yang, T. H.; Cao, D. K.; Li, Y. Z.; Zheng, L. M. *J. Solid State Chem.* **2010**, *183*, 1159–1164. (b) Guo, Y. Q.; Yang, B. P.; Song, J. L.; Mao, J. G. *Cryst. Growth Des.* **2008**, *8*, 600–605. (c) Jones, S.; Liu, H. X.; Schmidtke, K.; C. O'Connor, C.; Zubieta, J. *Inorg. Chem. Commun.* **2010**, *13*, 298–301. (d) Costantino, F.; Ienco, A.; Midollini, S. *Cryst. Growth Des.* **2010**, *10*, 7–10. (e) DeBurgomaster, P.; Ouellette, W.; Liu, H.; J. O'Connor, C.; Zubieta, J. *CrystEngComm.* **2010**, *12*, 446–469.

(6) (a) Zhu, Y. Y.; Sun, Z. G.; Tong, F.; Liu., Z. M.; Huang., C. Y.; Wang, W. N.; Jiao, C. Q.; Wang, C. L.; Li, C.; Chen, K. *Dalton Trans.* **2011**, *40*, 5584–5590. (b) Liu, L.; Sun, Z. G.; Zhang, N.; Zhu, Y. Y.; Zhao, Y.; Lu, X.; Tong, F.; Wang, W. N.; Huang, C. Y. *Cryst. Growth Des.* **2010**, *10*, 406–413. (c) Zhu, Y. Y.; Sun, Z. G.; Chen, H.; Zhang, J.; Zhao, Y.; Zhang, N.; Liu, L. *Cryst. Growth Des.* **2009**, *9*, 3228–3234. (d) Zhu, Y. Y.; Sun, Z. G.; Zhao, Y.; Zhang, J.; Lu, X.; Zhang, N.; Liu, L. *New J. Chem.* **2009**, *33*, 119–124.

(7) Liu, X. G.; Huang, J.; Bao, S. S.; Li, Y. Z.; Zheng, L. M. *Dalton Trans.* **2009**, 9837–9842.

(8) Tong, F.; Sun, Z. G.; Chen, K.; Zhu, Y. Y.; Wang, W. N.; Jiao, C. Q.; Wang, C. L.; Li, C. *Dalton Trans.* **2011**, *40*, 5059–5065.

(9) Serre, C.; Stock, N.; Bein, T.; Férey, G. *Inorg. Chem.* **2004**, *43*, 3159–3163.

(10) Sheldrick, G. M. *Acta Crystallogr., Sect. A.* **2008**, *64*, 112–122.

(11) Du, Z. Y.; Sun, Y. H.; Zhang, X. Z.; Luo, S. F.; Xie, Y. R.; Wan, D. B. *CrystEngComm.* **2010**, *12*, 1774–1778.

(12) Fang, C. Y.; Chen, Z. X.; Liu, X. F.; Yang, Y. T.; Deng, M. L.; Weng, L. H.; Jia, Y.; Zhou, Y. M. *Inorg. Chim. Acta* **2009**, *362*, 2101–2107.

(13) Sun, Z. M.; Mao, J. G.; Sun, Y. Q.; Zeng, H. Y.; Clearfield, A. *New J. Chem.* **2003**, *27*, 1326–1330.

(14) Cabeza, A.; Aranda, M. A. G.; Bruque, S. *J. Mater. Chem.* **1998**, *8*, 2479–2485.

(15) Song, J. L.; Lei, C.; Sun, Y. Q.; Mao, J. G. *J. Solid State Chem.* **2004**, *177*, 2557–2564.

(16) (a) Cabeza, A.; Ouyang, X.; Sharma, C. V. K.; Aranda, M. A. G.; Bruque, S.; Clearfield, A. *Inorg. Chem.* **2002**, *41*, 2325–2333. (b) Sun, Z. M.; Mao, J. G.; Yang, B. P.; Ying, S. M. *Solid State Sci.* **2004**, *6*, 295–300.

(17) Li, J.; Ji, C. C.; Huang, L, F.; Li, Y. Z.; Zheng, H. G. *Inorg. Chim. Acta* **2011**, *371*, 27–35.

(18) Yang, J.; Li, G. D.; Cao, J. J.; Yue, Q.; Li, G. H.; Chen, J. S. *Chem.—Eur. J.* **2007**, *13*, 3248–3261.

(19) Hu, J. Y.; Zhao, J. A.; Hou, H. W.; Fan, Y. T. *Inorg. Chem. Commun.* **2008**, *11*, 1110–1112.